

Ming Cui
Peter Wonka
Anshuman Razdan
Jiuxiang Hu

A new image registration scheme based on curvature scale space curve matching

Published online: 22 June 2007
© Springer-Verlag 2007

M. Cui (✉) · P. Wonka
Department of Computer Science and
Engineering, Prism, Arizona State
University, 878609, Tempe, AZ
85287-9909, USA
ming.cui@asu.edu

A. Razdan · J. Hu
P³DEA, Arizona State University at
Polytechnic Campus, 7001 E. Williams
Field Rd. Bldg. 140, Mesa, AZ 85212,
USA

Abstract We propose a new image registration scheme for remote sensing images. This scheme includes three steps in sequence. First, a segmentation process is performed on the input image pair. Then the boundaries of the segmented regions in two images are extracted and matched. These matched regions are called confidence regions. Finally, a non-linear optimization is performed in the matched regions only to obtain a global set of transform parameters. Experiments show that this scheme is more robust and converges faster

than registration of the original image pair. We also develop a new curve-matching algorithm based on curvature scale space to facilitate the second step.

Keywords Image registration · Curve matching · Curvature scale space

1 Introduction

Image registration is a fundamental problem in image processing and often serves as an important preprocessing procedure for many applications such as image fusion, change detection, super resolution, and 3D reconstruction. While we can draw from a large number of solutions [5, 46], most existing methods are specifically tailored to a particular application. For example, video-tracking focuses on non-rigid transformations with small displacements and medical image registration can take advantages of the uniform background and absence of occlusion. In this paper, we work with remote sensing image pairs that have been geometrically and photometrically rectified to some extent and differ by a global similarity transform. The output of the computation is the set of global parameters of the transform.

In the scope of remote sensed image registration existing methods fall into two categories: area-based methods and feature-based methods [46]. Area-based methods [21, 45] directly use the whole image or some predefined win-

dows without attempting to find salient features. First, a function is defined, such as correlation or mutual information, to evaluate the similarity between the image pairs under a given transformation. The second step is an optimization procedure to find the parameter set that maximizes the function. The drawback of this approach is twofold: searching for a global optimum is computationally expensive and the search space is not smooth due to non-overlapping areas and occlusion in the input images. Therefore, the search process will probably stop at a local optimum instead of a global optimum. In contrast, feature-based methods determine the transformation by matching salient features extracted from the original image pairs. The difficulty of these algorithms is to find corresponding features robustly. If features are matched incorrectly, they become outliers. As features only draw from a smaller local region, the algorithms might create a large number of such outliers and the elimination of outliers is very time consuming and unstable.

We propose a new registration scheme that is a combination of these two approaches: The first step is to segment

the input images and to extract closed boundary curves. The second step is to match the extracted curves by an improved curvature scale-space algorithm. In the third step, we try to register the two images using only the regions enclosed by the matched boundaries with an area-based method. This registration framework compares favorably to using feature-based registration or area-based registration alone. Because we use curves as geometric features, our feature-based matching algorithm is more robust than relying on point features. Additionally, the curve-based feature-matching algorithm identifies potentially matched regions. This helps the area-based optimization algorithm in the following ways: a) curve matching gives multiple initial guesses to start a local optimization algorithm. b) The search space is smoother compared to the search space induced by the original image pair and therefore there are less chances of getting stuck in a local optimum. c) The computational overhead is greatly reduced. We will demonstrate these advantages through experiments on selected data sets.

The paper is organized as follows: Sect. 3 gives an overview of the registration scheme. Section 4 details the curve extraction and curve matching steps of the framework. Section 5 explains the area-based registration step. Section 6 gives the results of our implementation on selected test data sets. Section 7 provides concluding remarks and outlines ideas for future work.

2 Related work

2.1 Image registration

Image registration techniques can be categorized according to their application area [6, 17, 24]. The most prominent areas are medical imaging, remote sensing, and computer vision applications such as video registration. For medical images, the objects under registration often go through non-rigid deformation, therefore non-rigid registration methods [27] such as diffusion-based methods [35] and level set methods [40] are very popular. In [31] the state of the art of video registration is demonstrated. In remote sensing image registration, the methods described in [25, 28] are representative. In this area both feature-based methods and area-based methods are useful. In the methods described in [11, 14, 40] features invariant to a selected transform are first extracted and matched. Remote sensing images often contain many distinctive details that are relatively easy to detect (point features, line features, region features). Wavelet decomposition and multi-resolution [26] techniques are often involved to make the procedure more effective and efficient. Methods based on template matching [13] can help with images that are not radiometrically rectified. Methods using mutual information [10, 12, 39, 42] are also introduced to deal with multi-modal image registration.

2.2 Curve matching

We use a curve (shape) matching algorithm based on the curvature scale space descriptor (CSSD) [23, 29] to facilitate the registration process. CSSD is a shape representation and description technique aimed to effectively capture important shape features based on either boundary information or the interior content information of the target shapes. Other shape description methods include shape signature, such as the chain code [34] and moments [4], the Fourier descriptor [9], the medial axis transform [33], and the shape matrix [16]. Researchers have found that shape description and matching techniques are very useful for remote sensing image registration. Thus different shape description methods have been adopted to aid registration, such as the improved chain code [11], moments [15] and the shape matrix [3]. It has been generally recognized that CSSD is a good shape description method because it can provide a multi-scale representation for the shape and the extracted features have good perceptual significance. However, the CSSD matching algorithm is very complex and sensitive to noise and partial occlusion. It also includes several ad-hoc parameters to adjust for different inputs, which makes it not robust. In this article, we suggest a new matching algorithm, which is more robust and has no ad-hoc parameters to alleviate these shortcomings. Furthermore, we are the first to use curvature scale space for image registration.

3 Overview

The new registration scheme consists of three building blocks, as shown in Fig. 1. The details of these building blocks will be discussed in subsequent sections. In this overview section we will mainly focus on the input and output of each block, and how they cooperate to make the whole scheme work:

Segmentation. The first building block is segmentation. Segmentation requires a gray scale image as input and computes a set of non-intersecting closed regions. The boundaries of these regions are closed curves. These closed curves are the output of this building block. Ideally, the segmentation finds some salient regions that correspond to meaningful physical objects in the remote sensing images, such as lakes, forests, or regions separated by road networks or rivers. The requirement for the segmentation algorithm is that it be able to pick up several of these outlines. Currently, we use a modified watershed transform for the segmentation algorithm.

Curve matching. The input of the curve matching algorithm is a set of curves extracted from image 1 and another set of curves extracted from image 2. The as-

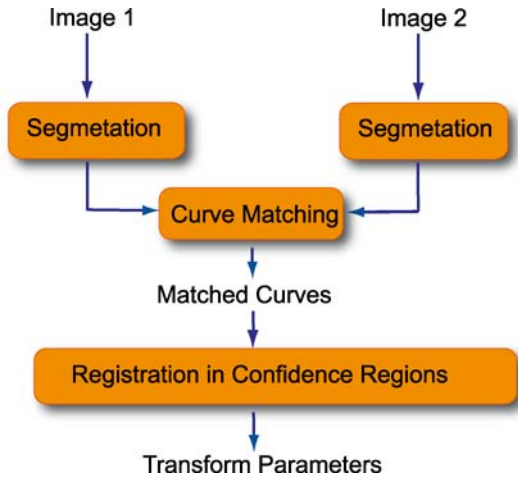


Fig. 1. Overview of our registration algorithm consisting of three major parts. The first part is a segmentation algorithm that extracts closed curves from the two input images. The second part is a curve matching algorithm that computes a set of matched curve pairs. The third part is an area-based registration algorithm that computes the final result by iterative optimization of a similarity metric in selected confidence regions

sumption of the curve matching algorithm is that the same physical objects will have very similar outlines if they appear in both input images. The curve-matching step tries to match outlines that correspond to the same physical objects. The algorithm computes the similarity between each possible pair of curves. A valid pair consists of one curve stemming from image 1 and another curves stemming from image 2. The output of the curve matching is a set of N curve pairs with the highest similarity. The number N is decided by the user or some similarity criterion. We call the regions inside the matched curves potentially matched or confidence regions. Along with each matched pair, a gross estimation of the transform is also included in the output. The algorithm we use is an improvement of the curvature scale-space algorithm.

Area-based registration. The input to the area-based registration step is: a) the two original input images, b) the potentially matched regions, including c) the estimates of the transform parameters. The output of the registration step is the optimal set of transform parameters obtained by a non-linear optimization process. The optimization process consists of an algorithm to search for a local optimum near a given point in the search space. This algorithm is invoked several times using the initial guesses obtained by the curve-matching step. How many local optimizations are performed can be decided by a user-defined number M . Alternatively, all initial guesses can be used. The registration algorithm conducts the optimization only in the confidence regions to improve performance.

4 Feature matching

4.1 Segmentation and curve extraction

The segmentation step plays a significant role in the resulting registration. Currently, we work with existing segmentation methods. We employ a modified watershed transform [32]. As observed by other researchers in this field, current segmentation methods have certain weaknesses: a) almost all segmentation algorithms have parameters that need to be adjusted for different input images. b) Segmentation is sensitive to noise, shadows, occlusion, etc. The second problem is hard to address in general. However, since we are dealing with aerial images that are already rectified and differ only by a similarity transform this problem is partially alleviated. While our implementation shows that using current segmentation methods allows for strong registration results, we need a curve-matching algorithm that is able to overcome some of the shortcomings of the segmentation. Therefore, our curve-matching scheme is designed in such a way, that it tolerates noise and partial deterioration of curves. Additionally, the complete registration framework will still be functional if some curves are matched incorrectly. The segmentation algorithm gives a decomposition of the image into labeled regions. We extract boundary curves in the form of lists of two-dimensional points [4] and pass these point lists to the curve-matching algorithm.

4.2 Curve matching

The core idea behind the matching algorithm is that two curves representing the same physical object will differ only by a similarity transform, which includes uniform scaling, rotation and translation. Therefore, we need to use a description of a curve that is invariant to the similarity transform. Further, we need a robust algorithm that compensates for noise in the segmentation process. Our algorithm uses the curvature scale space descriptor to represent and match boundary curves. This representation is invariant to the similarity transform and provides the basis for a robust matching algorithm. We will first explain the curvature scale space descriptor. Then we will give the details of our new matching algorithm to estimate the similarity between two curves and finally describe how this curve-matching algorithm can be used to match two sets of curves.

The curvature scale space image (CSSI) [23] is a binary two-dimensional image that records the position of inflection points of the curve convoluted by different-sized Gaussian filters. A planar curve r is given as a polyline defined by a set of discrete points. This curve can be represented by the parametric vector equation with parameter u , where x and y describe the coordinate values:

$$r(u) = (x(u), y(u)). \quad (1)$$

From the original curve, a set of curves is created by low-pass Gaussian filtering with a different kernel size parameter σ :

$$\Gamma_\sigma = \{(X(u, \sigma), Y(u, \sigma)) | u \in [0, 1]\}, \quad (2)$$

where $(X(u, \sigma) = x(u) * g(u, \sigma)$ and $Y(u, \sigma) = y(u) * g(u, \sigma)$. Convolution is denoted by $*$ and

$$g(u, \sigma) = \frac{1}{\sigma\sqrt{2\pi}} e^{-\frac{u^2}{2\sigma^2}}. \quad (3)$$

Each curve in the set will create one row of the scale space image by the following method: the parameter u is discretized and for each value of u the curvature k can be estimated by the following equation:

$$k(u) = \frac{\dot{x}(u)\ddot{y}(u) - \dot{y}(u)\ddot{x}(u)}{(\dot{x}(u)^2 + \dot{y}(u)^2)^{\frac{3}{2}}}. \quad (4)$$

If the curve with a smoothing parameter has a zero crossing in curvature at location u we set $CSSI(\sigma, u) = 1$ and $CSSI(\sigma, u) = 0$ otherwise. A zero crossing in curvature is an indicator of a significant feature in the curve. This indicator is invariant to affine transformations. See Fig. 2, left, for an example of a curve and its curvature scale space image.

Given two curves the respective CSSIs are great representations for curve matching. The conventional CSSI matching algorithm [29] first tries to align the CSSIs to compensate for the difference in orientation. Such an alignment can be done by computing the appropriate circular horizontal shift of the image. The original algorithm is based on an analysis of the highest and second highest contour maximum. However, this algorithm has some problems [8, 44] that we try to overcome.

- The algorithm relies on the extraction of contour maxima. In practice, the CSSI will often be non-continuous and have several close-by maxima. As a result the maximum extraction is unstable, time consuming, and requires the specification of ad-hoc parameters. In con-

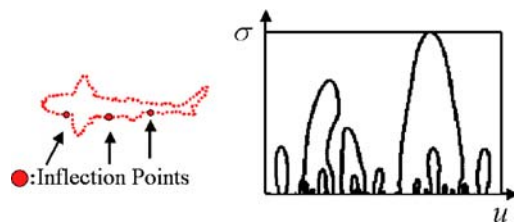


Fig. 2. *Left:* a closed curve depicting the outline of a fish. Inflection points are shown in red. *Right:* the scale space image of the curve to the left. Each row of the scale space image corresponds to a curve of scale σ that is parameterized by $u \in [0, 1]$. The black entries record the inflection point for one scale determined by the smoothing parameter of the Gaussian filter σ

trast, the idea of our algorithm is to avoid the detection of contour maxima to improve stability.

- To increase stability of maximum extraction, the original algorithm used small increments for the support of the Gaussian filter σ . This results in CSSIs with a large number of rows. Our algorithm works with increments that are one order of magnitude larger so that we only need to compare relatively small CSSIs.
- To compute the circular shift parameter between two curves would require an exhaustive search that is overly time consuming for most applications. The original algorithm proposes an acceleration that only examines four distinct shift parameters. For curves that have partial deterioration this acceleration algorithm is very likely to fail. Our algorithm makes use of dynamic programming, so that we can find the global optimum of our similarity metric.

We propose a new CSS matching algorithm that has two new features: first, the whole CSSI is compared line by line in contrast to the conventional algorithm; second, dynamic programming is used to guarantee a global optimum.

First, we define a cost metric for comparing a line i in CSSI image 1 with a line j in CSSI image 2. As shown in Fig. 3, left, each line of the CSSI is a binary string with values of either 0 or 1. We warp this line into a circle and consider the position where values take 0 as empty and 1 as occupied by a small ball with unit mass. Then the centroid of all these small balls is calculated. We can estimate four parameters (two of them are shown in Fig. 4):

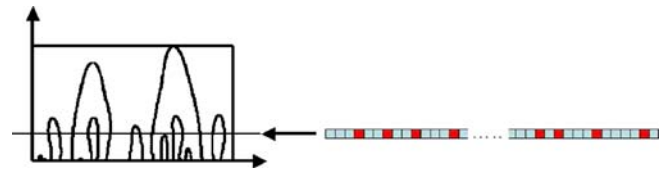


Fig. 3. CSSI (scale space curvature image). Each line is a binary string

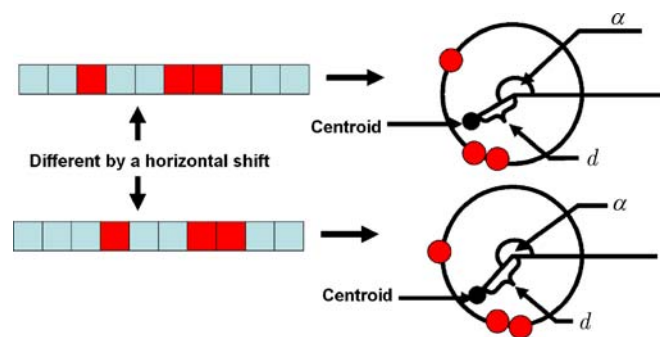


Fig. 4. Comparing two lines of a CSS image

the angle α spanned by the connecting line and a reference horizontal line, the distance d between the centroid and the center of the circle, the mass m computed by the number of 1s in the line, and the standard deviation std . The main reason we chose these features is that they are a good description of the distribution of the inflection points and are invariant to circular rotation (circular shift). Additionally, higher order moments could be used, but that was not stable in our experiments. We use three features to establish a cost metric c that compares a line i in CSSI 1 with line j in CSSI 2. We use only three of the features in this formula. The use of the angle feature and the parameter values for λ_i will be explained later in the dynamic programming step.

$$c(i, j) = \lambda_1|m_i - m_j| + \lambda_2|d_i - d_j| + \lambda_3|std_i - std_j|. \quad (5)$$

Using this metric c to compare two single lines i and j , a dynamic programming [41] process is used to find the total cost TC between two curves' CSSIs. The difficulty arises from the fact that we cannot simply compare all pairs of lines with the same index i . The intrinsic properties of CSSI images suggest that we have to consider non-linear scaling along the scale axis of the CSSIs in the total cost TC [1]. Dynamic programming [2] is a perfect match for this task, as it allows comparison of lines across different scales. The first step of dynamic programming is to build a cost table. Each row of the table corresponds to a line of CSSI 1 and each column corresponds to a line of CSSI 2. A cell in the cost table contains the cost $c(i, j)$ described above (see Fig. 7). The second step is to build an aggregated cost table as follows: $ac(1, 1) = c(1, 1)$ and

$$ac(i, j) = c(i, j) + \min \begin{cases} ac(i-1, j) + \lambda_4||\alpha_{i-1} - \alpha_j| - |\alpha_i - \alpha_j|| \\ ac(i, j-1) + \lambda_4||\alpha_i - \alpha_{j-1}| - |\alpha_i - \alpha_j|| \\ ac(i-1, j-1) + \lambda_4||\alpha_{i-1} - \alpha_{j-1}| - |\alpha_i - \alpha_j|| \end{cases}$$

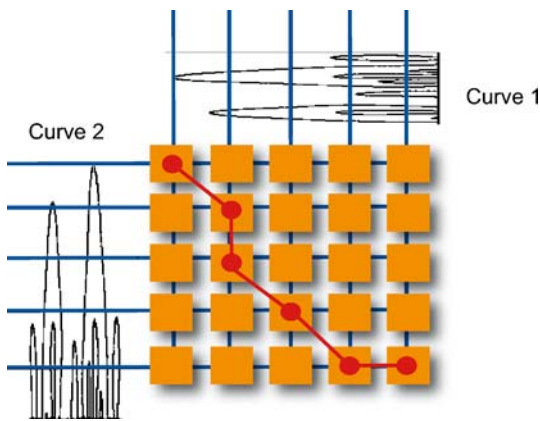


Fig. 5. Overview of dynamic programming for comparing two curves

The aggregate cost function of every cell is composed of two parts: 1) the distance of the matching two rows (scales) of CSSIs that intersect at this cell and 2) an angle-dependent cost related to the absolute difference between the angle at this cell and the previous cell. The second part of the cost function means that we do not restrict the comparison to finding one global horizontal shift, but we allow small variations between neighboring cells. However, we penalize large differences in angle to only allow minor differences. The angle-dependent cost will then be multiplied by a weight factor λ_4 . The total cost of matching the two curves can then be found in the bottom right cell $TC = ag(i_{max}, j_{max})$. Because we do not use contour maximum detection as the original algorithm our technique is stable even with large increments of the Gaussian filter support σ . Therefore, the table size is fairly small and we did not optimize the search process for the global optimum. We obtained table sizes of 10×10 up to 20×20 in our results. The table size is implicitly determined by the complexity of the curve. Through experiments we found $\lambda_1 = 0$, $\lambda_2 = 1$, and $\lambda_3 = 0.3$, and $\lambda_4 = 1$ to provide the best results. Alternatively, we experimented with a version that had higher weight λ_4 at lower resolution. The idea is that higher resolutions are more likely to be subject to noise and we want to decrease the effect of noise in the overall similarity metric. While this idea resulted in minor changes in curve matching, it did not influence the outcome of the registration for any image pair. Even though the CSSI matching algorithm compares complete curves,

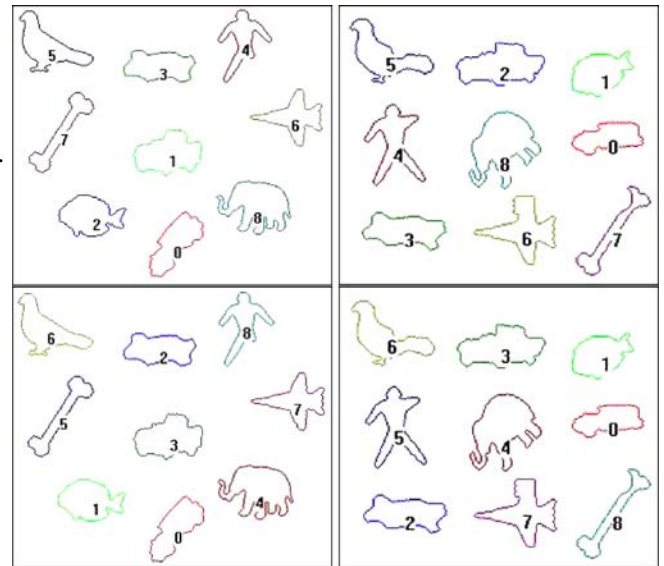


Fig. 6. The results of the curve matching algorithm on the Kimia shape database. Top row: a curve matching result for the standard CSS algorithm. Second row: our results. Each row contains the same image pair with nine shapes per image. The label assignment is computed by the curve matching algorithms. Note that both algorithms misclassify two shapes

it can also match curves with partial correspondence [30]. This is shown in Fig. 6.

The output of the dynamic programming algorithm is a similarity between two curves. Using this algorithm as a building block, our next task is to find the best matches between two sets of curves. Suppose m and n curves are extracted from two images, respectively, then the costs of each possible match is evaluated. These costs form a matrix. If $l = \min(m, n)$, then we want to find l curve pairs that will minimize the overall cost. We further restrict the matching to allow each curve to appear only in one curve pair. This is an example of an assignment problem. We solve this problem with the Hungarian method [19].

4.3 Complexity analysis

The complexity of the original curve matching algorithm and our new algorithm is similar. Suppose the input curves have M discrete points and the Gaussian filter has N levels. The size of the CSSI will be $M * N$. In the original algorithm, the whole CSSI has to be scanned once to find all the contour maxima. This step is $O(MN)$. The contour maxima will be stored as a feature list. We assume the feature list will have the size $\log(M)$. Then a circular shift will be performed to align the highest maxima in the two CSSIs. For each feature in the first list, the second list will be scanned to find the nearest feature. Then a circular shift will be performed to align the highest maxima in the first CSSI to the second highest maxima and repeat the following operations. Overall, the complexity of the original curve-matching algorithm will be $O(MN + \log(M)^3)$. In our algorithm, the CSSI will also be scanned once to decide the shift angle and distance for each row. Then the dynamic programming will have a constant complexity of $N * N$. The overall complexity will be $O(MN + N^2)$. Since N is usually much smaller than M , the complexity is comparable. Our results in Sect. 6 also show comparable running speeds of the implementation.

5 Area-based registration

We adopt a general parametric registration framework that is illustrated in Fig. 7. We have two input images: one is selected as the reference image and the other one is the moving image. We estimate initial transform parameters for each matched curve pair and then run the local optimization process. The best result is returned as the global optimal set of parameter.

5.1 Local optimization

We use an iterative optimization process to find the best local transform parameters. At each step of the optimization, the moving image is transformed by the current transform parameters and resampled on the reference image's

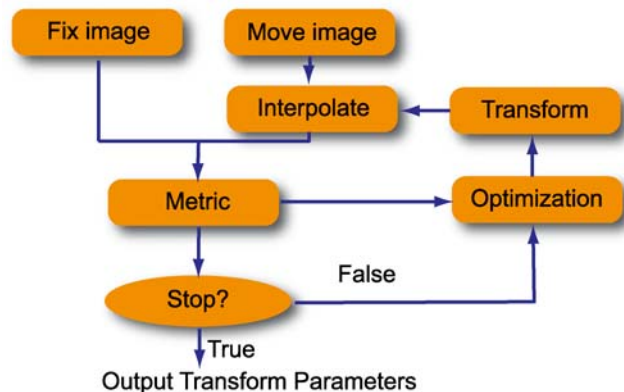


Fig. 7. Overview of the complete registration framework

grid. We implemented two different resampling schemes: nearest neighbor interpolation and bilinear interpolation (bilinear interpolation is used in the results section). After the two images are aligned we compute the set of pixel locations Ω that are inside confidence regions in both input images. A similarity value can then be computed using either a mean square metric, a mutual information metric, or normalized cross correlation. The mean square metric,

$$MS(R, M) = \frac{1}{N} \sum_{i \in \Omega} (R_i - M_i)^2 \quad (6)$$

calculates the L_2 norm of the intensity differences. The mutual information metric,

$$MI(R, M) = \int_R \int_M p(x, y) \log \frac{p(x, y)}{p(x)p(y)} dx dy \quad (7)$$

compares the probability density function of the separate and joint distribution for each intensity pair. The normalized cross-correlation

$$NC(R, M) = \frac{\sum_{i \in \Omega} (R_i M_i)}{\sqrt{\sum_{i \in \Omega} (R_i^2) \sum_{i \in \Omega} (M_i^2)}} \quad (8)$$

is another similarity metric that is similar to the mean square metric, but it is insensitive to scaling the intensity of one or both images with a multiplicative factor. We use a gradient descent method for the optimization process, because we already have an initial estimate. Our implementation follows the description in the book *Introduction to Optimization* [43], pp. 115–122. More complicated global search strategies exist, such as genetic algorithms [7], simulated annealing [18] and stochastic gradient algorithms [20]. These strategies are used in case the initial guess is far from the global optimum. In contrast, our registration scheme computes a good initial estimate through geometric curve matching and smoothes

the search space through the use of confidence regions to make a local search sufficient. Given a matched curve pair, we can estimate an initial guess for the transform as follows: 1) The translation parameter is estimated by the difference between the centroids of the two regions. 2) The scaling parameter can be estimated by the difference between the areas of the matched regions. 3) The rotation parameter is estimated by the circular horizontal shift between the two matched curve's CSSI.

6 Results

In this section we evaluate the curve matching algorithm and the complete image registration framework on selected test cases.

To evaluate the curve matching algorithm we use eight test cases. The first two are selected curves from the Kimia shape database [38]. The other six are sets of curves extracted from aerial images. We compare our curve matching algorithm to three other algorithms: the

original CSS algorithm [29], the original Fourier descriptor methods [9], and a recent improved Fourier descriptor method [22]. The results are shown in Table 1. We can see that our method outperforms all other methods in terms of matching performance with all methods having similar running times. As we will show below we can improve the performance even more by increasing the sampling resolutions of the curves. It is important to note that neither of the Fourier descriptor methods can improve the performance with more expensive settings. To give a visual

Table 1. This table compares our improved CSSI-based curve matching algorithm with three other published algorithms. FD1 is the original Fourier descriptor method and FD2 is a recent improvement of Fourier descriptors. OCSS denotes the original scale space algorithm and NCSS is our new method described in this paper

	Correct matches				Time in s			
	FD1	FD2	OCSS	NCSS	FD1	FD2	OCSS	NCSS
test1	7/9	9/9	7/9	7/9	1.4	1.5	1.8	1.7
test2	5/8	4/8	5/8	5/8	2.0	2.0	2.5	1.7
test3	6/6	6/6	4/6	6/6	1.2	1.3	2.2	1.5
test4	9/9	9/9	6/9	9/9	1.1	1.1	2.1	1.1
test5	9/9	4/9	9/9	7/9	1.3	1.4	2.2	1.9
test6	4/7	7/7	5/7	7/7	1.4	1.8	2.1	2.0
test7	4/6	6/6	4/6	6/6	1.1	1.1	1.9	1.4
test8	7/9	7/9	7/9	7/9	1.4	1.2	2.4	1.4
total	80%	84%	74%	87%	11	11.4	17.2	12.7

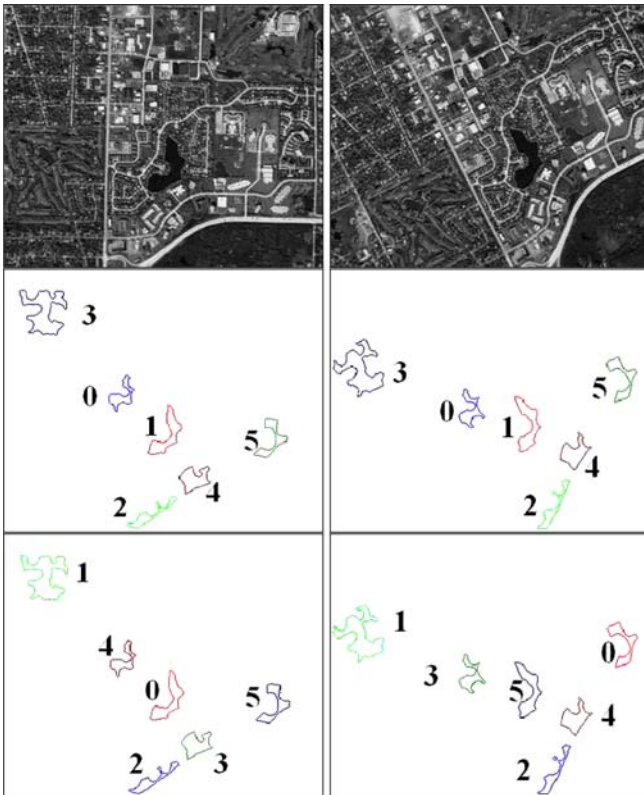


Fig. 8. Results of the curve-matching algorithm for real aerial images. *First row:* the original image pair. *Second row:* the result of our curve matching algorithm. The extracted curves are shown for both images. The computed pairing is indicated by the numbers next to the curves. *Third row:* result of the original curve matching algorithm

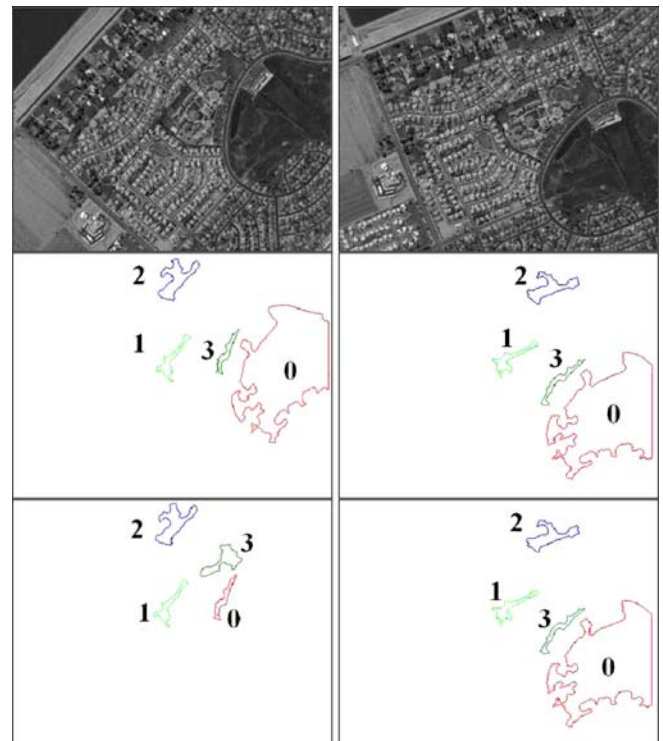


Fig. 9. See Fig. 8

impression of our test cases and results, we show three examples: curves from the Kima shape database used in *test1* (see Fig. 6) and curves extracted from aerial images used in *test3* (see Fig. 8) and *test4* (see Fig. 9).

We conducted other tests and varied the two most important parameters of the curve matching algorithm: the sampling resolution and the number of features used. We evaluated the influence of the sampling resolution sr along the arc-length of a curve by comparing the settings 64, 128, 256, and 512 (setting 128 is used for all other tests in this paper). We also changed the number of features that we used to describe a line in the CSSI. The main method uses three features: angle, first moment, and second moment. This setting corresponds to the columns where $F = 3$. We compare this setting to $F = 4$ where we add the mass (zeroth moment) and $F = 2$ where we drop the second moment. The features are described in Sect. 4. The results of the comparison are given in Table 2. Please note that our method can improve the matching perform-

ance with a higher sampling resolution of 256 and that the algorithm performs best with three features.

To evaluate the complete registration framework, we compare our registration scheme to four other methods: *Sift*—probably the most popular feature based method [36], *UCSB* [37]—registration with fit assessment, a different variation of feature-based matching, *Area MS* [6]—an area-based method using the mean squares as metric, and *Area MI* [12, 42]—an area-based method using mutual information. We also show results for two settings of our new algorithm. The main method *MM* uses mean squares as a matching function and *NC* uses normalized cross correlation. We also tested the mutual information metric, but this version of our algorithm sometimes does not have enough sample points inside the confidence regions to work well. We created a test suite of 11 image pairs. Figures 8, 9, and 12 show image pairs 1, 2, and 3 respectively. The image pairs 4, 5, 6, and 7 are shown in Fig. 13. The image pairs 8,9,10,and 11 are shown in

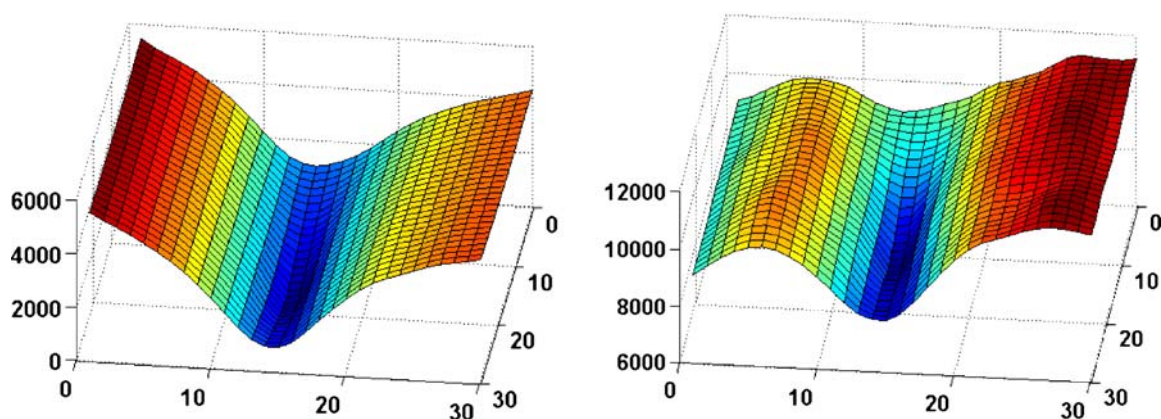


Fig. 10. Visualization of the search space spanned by the rotation and scaling parameters. *Left:* search space spanned by confidence regions. *Right:* search space of the original image. Note that the confidence regions result in a smoother search space

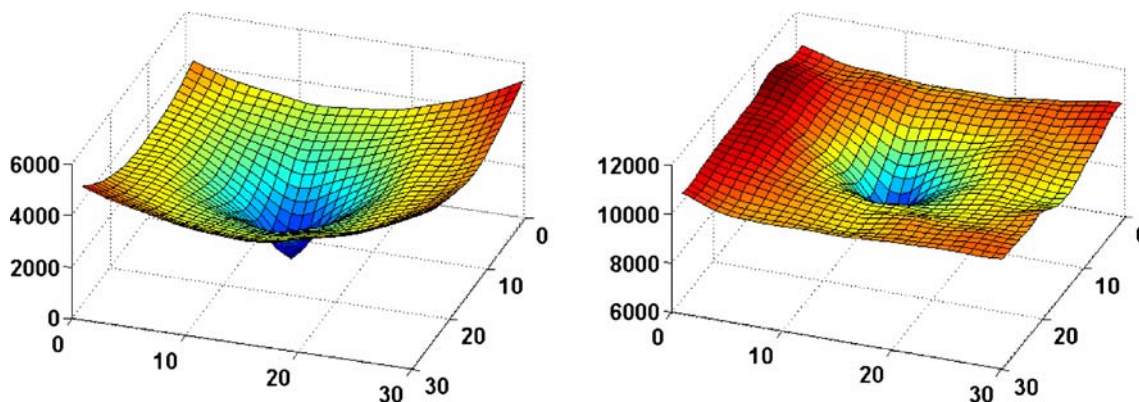


Fig. 11. Visualization of the search space spanned by the translation parameters. *Left:* search space spanned by confidence regions. *Right:* search space of the original image. Note that the confidence regions result in a smoother search space

Table 2. Comparison of various parameter settings for the curve matching algorithm. Combinations of four different sampling resolutions 64, 128, 256, and 512, with different combinations of used features, are compared. $F = 2$ only uses distance and angle, $F = 3$ uses the second moment as additional feature, and $F = 4$ additionally uses mass. Note that the more expensive resolution 256 clearly outperforms fourier descriptors (see Table 1)

	Correct matches						Time in s					
	64	$F = 3$		512	$F = 2$	$F = 4$	64	$F = 3$		$F = 2$	$F = 4$	
		128	256		128	128		128	256	512	128	128
test1	7/9	7/9	7/9	7/9	7/9	7/9	1.2	1.7	4.7	11.1	1.6	1.7
test2	2/8	5/8	5/8	5/8	4/8	5/8	1.1	1.7	4.9	9.6	1.7	1.7
test3	6/6	6/6	6/6	6/6	6/6	6/6	1.3	1.5	4.4	8.5	1.6	1.9
test4	7/9	9/9	9/9	6/9	9/9	7/9	1.1	1.1	3.7	5.7	1.1	1.1
test5	5/9	7/9	9/9	9/9	7/9	6/9	1.5	1.9	5.2	9.3	1.9	2.3
test6	4/7	7/7	7/7	7/7	4/7	7/7	1.6	2	6.1	10.5	2.1	2.6
test7	2/6	6/6	6/6	6/6	3/6	6/6	1.3	1.4	4.5	6.7	1.3	1.4
test8	4/9	7/9	9/9	9/9	7/9	7/9	0.9	1.4	3.9	6.1	1.4	1.4
total	59%	87%	93%	88%	74%	83%	10.0	12.7	37.4	67.5	12.7	14.1

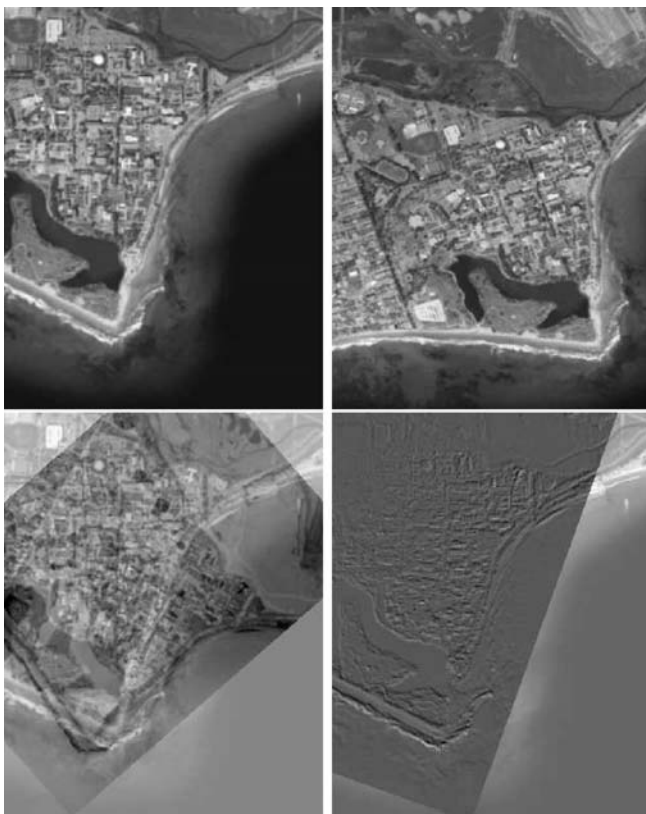


Fig. 12. First row: input images. Second row: left, result of an area-based method; right, result of our method. To show the visual result for the registration, the second input image is laid on the first one through the transform that we obtained from the corresponding algorithm. Then the intensity difference is calculated pixel by pixel. If the difference is equal to zero, the corresponding pixel in the result image is set to 125, which is gray. If the difference is 255, it is set to 255. If the difference is -255 , it is set to 0. Other values can be interpolated linearly. If the two images are perfectly registered, then the overlapping part result image should be uniformly gray

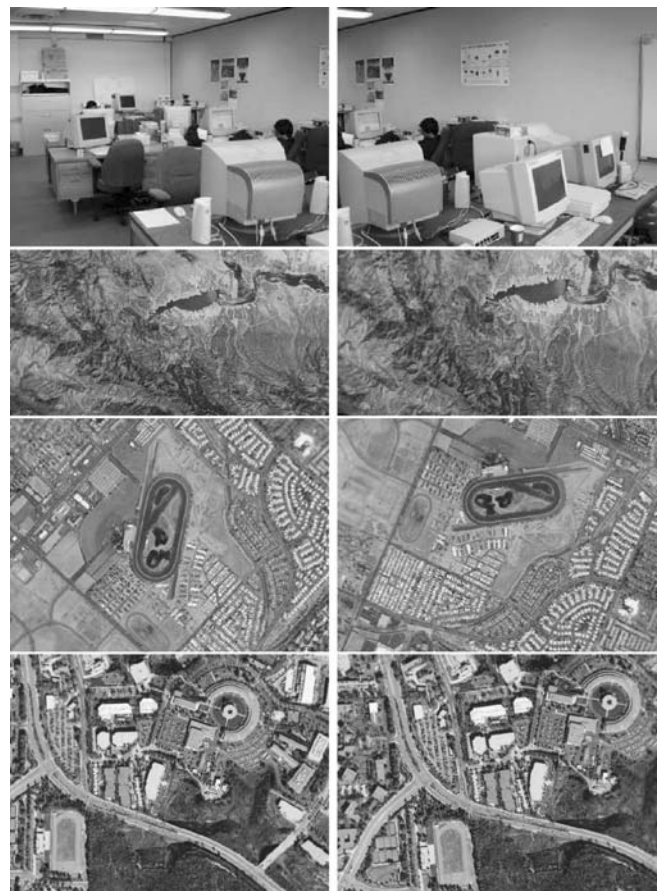


Fig. 13. Several image pairs from our test suite not shown in other figures

Fig. 14. The most important evaluation is a visual comparison of the matching result. Typically, all of the methods provide either excellent results, or results that are totally off, which makes visual matching easy (see Fig. 12 for an example). In the tests we recorded if a method was

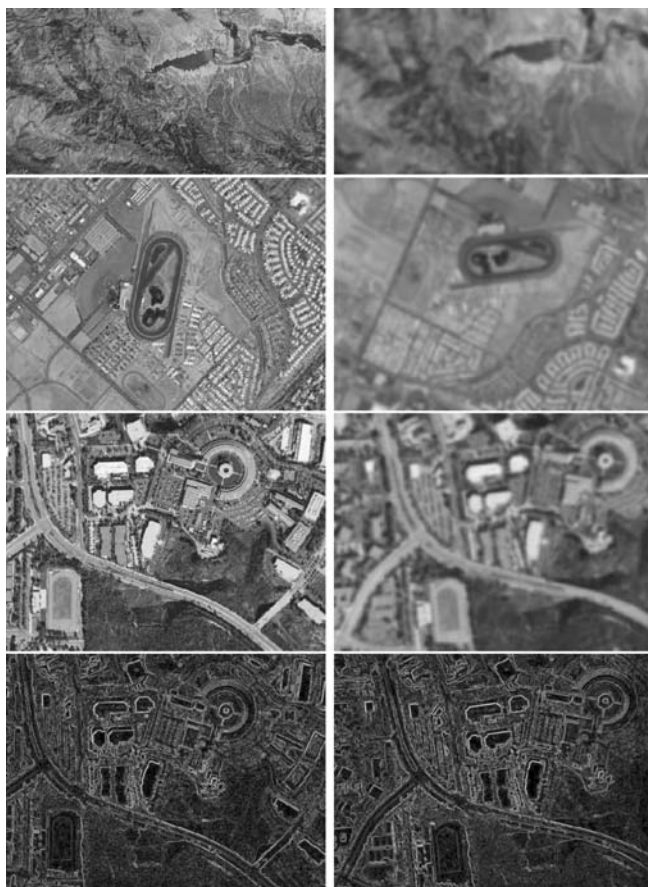


Fig. 14. Several image pairs from our test suite not shown in other figures

able to find the right transformation and how much time the computation took. The results are given in Table 3. Please note that we cannot report meaningful times for the *UCSB* method, because it was used over a web interface. The results show that feature-based methods are much stronger than area-based ones. However, we can see that the feature based methods are not able to cope with blurred images, while our new algorithm is still successful. The downside of our approach is that it does not work well with gradient images, such as the one selected in our test case.

Compared to the area-based methods, we have a much stronger initial estimate to start a local search. Additionally, the restriction to confidence regions results in a much smoother search space. We visualize the search space of the image pair in Fig. 8 in Figs. 10 and 11. Since high dimension space is hard to illustrate, we only show the space spanned by two parameters at one time; in Fig. 10 the space spanned by the rotation parameter and scaling parameter for fixed translation and in Fig. 11

Table 3. Comparison of multiple registration techniques. Two feature-based methods (Sift, UCSB), two area based methods (AREA MS, AREA MI) are compared with two versions of our new algorithm (MM, NC). The algorithms are described in the text. We report results on 11 image pairs by describing whether the registration was successful (y or n) and by reporting the computation time in seconds

	Correct y/n / Time in s					
	Sift	UCSB	A-MS	A-MI	MM	NC
test1	y 39	y 5	n 19	n 13	y 24	y 53
test2	y 31	y 5	y 200	y 76	y 57	y 77
test3	y 42	y 5	n 99	n 39	y 61	y 92
test4	y 35	y 5	n 52	n 23	y 6	y 41
test5	y 24	y 5	y 337	n 50	y 65	y 153
test6	y 19	y 5	n 431	n 37	y 44	y 110
test7	y 27	y 5	n 212	n 52	y 305	y 129
test8	n 22	n 5	n 122	n 70	y 17	y 80
test9	n 25	n 5	n 220	y 50	y 77	y 64
test10	n 33	n 5	n 230	n 31	y 32	y 26
test11	n 32	y 5	n 118	n 51	n 60	n 245

the space spanned by the translation parameter in X and Y directions.

7 Conclusions and future work

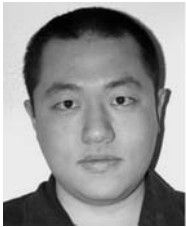
In this paper, the problem of remote sensing image registration was attacked. This paper makes two contributions to the state of the art in image registration. First, we introduced a new hybrid image registration scheme that combines the advantages of both area-based methods and feature-based methods. We extracted curves from the two input images through image segmentation and performed feature-based image registration: we compared and matched these curves to obtain several initial parameters for an area-based registration method. Then we used existing area-based methods in confidence regions to obtain a final result. This scheme allows us to combine feature-based and area-based registration in a robust and efficient manner. The second contribution of this paper is a new curve-matching algorithm based on curvature scale space to facilitate the registration scheme. We improved the matching algorithm of two scale space images and thereby the robustness and accuracy of the algorithm.

Currently our curve-matching algorithm works on the assumption that the same physical object will have the same shape contour in two input images. This is true for input images obtained from the same sensor and the same spectrum. However, in multi-spectral images the same physical object may have different shape contours in different spectral images. Our future work will focus on how to extend our registration scheme to multi-spectral image registration.

References

1. Abbasi, S., Mokhtarian, F., Kittler, J.: Enhancing CSS-based shape retrieval for objects with shallow concavities. *Image Vis. Comput.* **18**(3), 199–211 (2000)
2. Amini, A.A., Weymouth, T.E., Jain, R.C.: Using dynamic programming for solving variational problems in vision. *IEEE Trans. Pattern Anal. Mach. Intell.* **12**(9), 855–867 (1990)
3. Bentoutou, Y., Taleb, N., Kpalma, K., Ronsin, J.: An automatic image registration for applications in remote sensing. *IEEE Trans. Geoscience Remote Sensing* **43**, 2127–2137 (2005)
4. Boyle, R., Sonka, M., Hlavac, V.: *Image Processing, Analysis and Machine Vision*. Chapman & Hall, London (1998)
5. Brown, L.G.: A survey of image registration techniques. *ACM Comput. Surv.* **24**, 325–376 (1992)
6. Brown, L.G.: A survey of image registration techniques. *ACM Comput. Surv.* **24**(4), 325–376 (1992)
7. Chalermwat, P.: High-performance automatic image registration for remote sensing. PhD thesis, George Mason University (1999)
8. Chang, C.-C., Chen, I.-Y., Huang, Y.-S.: Pull-in time dynamics as a measure of absolute pressure. In: *Proceedings of the 16th International Conference on Pattern Recognition*, pp. 386–389. IEEE Computer Society (2002)
9. Chellappa, R., Bagdazian, R.: Fourier coding of image boundaries. *IEEE Trans. Pattern Anal. Mach. Intell.* **6**, 102–105 (1984)
10. Chen, H.-M., Varshney, P.K., Arora, M.K.: Performance of mutual information similarity measure for registration of multitemporal remote sensing images. *IEEE Trans. Pattern Anal. Mach. Intell.* **24**, 603–619 (2002)
11. Dai, X., Khorram, S.: A feature-based image registration algorithm using improved chain-code representation combined with invariant moments. *IEEE Trans. Geosci. Remote Sen.* **37**, 2351–2362 (1999)
12. Delaere, M.F., Vandermeulen, D., Suentens, D., Collignon P., Marchal, A., Marchal, G.: Automated multimodality image registration using information theory. In: *Proceedings of the 14th International Conference on Information Processing in Medical Imaging*, vol. 3, pp. 263–274. Kluwer Academic Publisher (1995)
13. Ding, L., Kularatna, T.C., Goshtasby, A., Satter, M.: Volumetric image registration by template matching. In: K.M. Hanson (ed.) *Proc. SPIE*, vol. 3979, pp. 1235–1246, *Medical Imaging 2000: Image Processing*, Kenneth M. Hanson; ed., Presented at the Society of Photo-Optical Instrumentation Engineers (SPIE) Conference, vol. 3979, pp. 1235–1246 (2000)
14. Flusser, J., Suk, T.: A moment-based approach to registration of images with affine geometric distortion. *IEEE Trans. Geosci. Remote Sen.* **32**, 382–387 (1994)
15. Fulong, C., Hong, Z., Chao, W.: A novel feature matching method in airborne sar image registration. In: *Geoscience and Remote Sensing Symposium, 2005. IGARSS'05. Proceedings*, pp. 4722–4724. IEEE Geoscience and Remote Sensing Society (2005)
16. Goshtasby, A.: Description and discrimination of planar shapes using shape features. *IEEE Trans. Pattern Anal. Mach. Intell.* **7**, 738–743 (1985)
17. Holden, M., Hawkes, D.J., Hill, D.L.G., Batchelor, P.G.: Medical image registration. *Phys. Med. Biol.* **46**, 1–45 (2001)
18. Johansson, M.: Image registration with simulated annealing and genetic algorithm. Master of Science Thesis, Stockholm, Sweden (2006)
19. Kuhn, H.W.: The Hungarian method for the assignment problem. *Nav. Res. Logist. Q.* **2**, 83–97 (1955)
20. LeMoigne, K.L., Zavorin, J., Cole-Rhodes, I., Johnson, A.A.: Multiresolution registration of remote sensing imagery by optimization of mutual information using a stochastic gradient. *IEEE Trans. Image Process.* **12**, 1495–1511 (2003)
21. Li, H., Manjunath, B.S., Mitra, S.K.: A contour-based approach to multisensor image registration. *IEEE Trans. Image Process.* **4**, 320–334 (1995)
22. Lu, G., Zhang, D.: A comparative study of Fourier descriptors for shape representation and retrieval. In: *Proc. of 5th Asian Conference on Computer Vision (ACCV)*. Asian Federation of Computer Vision Societies, Melbourne, Australia (2002)
23. Mackwoth, A., Mokhtarian F.: A theory of multi-scale, curvature-based shape representation for planar curves. *IEEE Trans. Pattern Anal. Mach. Intell.* **14**, 789–805 (1992)
24. Maintz, J., Viergever, M.: A survey of medical image registration. *Med. Image Anal.* **2**(1), 1–36 (1998). URL citeseer.ist.psu.edu/maintz98survey.html
25. Manjunath, B.S., Fonseca, L.M.G.: Registration techniques for multisensor remotely sensed imagery. *Photogramm. Eng. Rem. S.* **62**, 1049–1056 (1996)
26. McGuire, M., Stone, H.S., le Moigne, J.: The translation sensitivity of wavelet-based registration. *IEEE Trans. Pattern Anal. Mach. Intell.* **21**, 1074–1081 (1999)
27. McInerney, T., Terzopoulos, D.: Deformable models in medical images analysis: a survey (1996).
28. le Moigne, J.: First evaluation of automatic image registration methods. In: *Proceedings of the International Geoscience and Remote Sensing Symposium IGARSS98*, pp. 315–317. IEEE Geoscience and Remote Sensing Society, Seattle, Washington (1998)
29. Mokhtarian, F.: Silhouette-based isolated object recognition through curvature scale space. *IEEE Trans. Pattern Anal. Mach. Intell.* **17**, 539–544 (1995)
30. Mokhtarian, F., Bober, M.: *Curvature Scale Space Representation: Theory, Applications, and MPEG-7 Standardization*. Kluwer Academic Publishers, Norwell, MA (2003)
31. Mubarak Shah, R.K., (ed.): *Video Registration*. Kluwer, Boston (2003)
32. Pan, Y.H., Ming, C., Shou-Qian, S.: An image region merging algorithm based on modified fast watershed transform. *J. Comput.-Aided Design Comput. Graph., China* **17**, 546–552 (2005)
33. Pizer, S.M., Fletcher, P.T., Joshi, S., Thall, A., Chen, J.Z., Fridman, Y., Fritsch, D.S., Gash, A.G., Glotzer, J.M., Jiroutek, M.R., Lu, C., Muller, K.E., Tracton, G., Yushkevich, P., Chaney, E.L.: Deformable m-reps for 3D medical image segmentation. *Int. J. Comput. Vision* **55**(2–3), 85–106 (2003)
34. Saghi, A., Freeman, H.: Generalized chain codes for planar curves. In: *Proceedings of the Fourth International Joint Conference on Pattern Recognition*, pp. 701–703. Japan Institute of Electrical and Electronics Engineers, Kyoto, Japan (1978)
35. Thirion, J.P.: Image matching as a diffusion process: An analogy with Maxwell's demons. *Med. Image Anal.* **2**, 1–20 (1998)
36. UCLA: Sift implementation in matlab/c. <http://vision.ucla.edu/~vedaldi/code/sift/sift.html>
37. UCSB: Feature based registration platform. <http://nayana.ece.ucsb.edu/registration/>
38. University of Brown: Kimia shape database. <http://www.lems.brown.edu/vision/software/index.html>
39. Unser, M., Thevenaz, P., Ruttimann, U.E.: Iterative multiscale registration without landmarks. In: *Proceedings of the IEEE International Conference on Image Processing ICIP95*, pp. 228–231. Washington DC (1995)
40. Vemuri, B.C., Ye, J., Chen, Y., Leonard, C.M.: Image registration via level-set motion: Applications to atlas-based segmentation. *Med. Image Anal.* **7**(1), 1–20 (2003)
41. Wagner, D.B.: Dynamic programming. <http://citeseer.ist.psu.edu/268391.html>
42. Wells, W., Viola, P., Atsumi, H., Nakajima, S., Kikinis, R.: Multi-modal volume registration by maximization of mutual information (1996)

43. Zak, S.H., Chong, E.K.P.: An Introduction to Optimization. John Wiley, New York (2001)
44. Zhang, D., Lu., G.: Review of shape representation and description technique. *Pattern Recogn.* **37**, 1–19 (2004)
45. Zheng, Q., Chellappa, R.: A computational vision approach to image registration. *IEEE Trans. Image Process.* **2**, 311–326 (1993)
46. Zitova, B., Flusser, J.: Image registration methods: A survey. *Image Vis. Comput.* **21**, 977–1000 (2003)



MING CUI received his BE in Civil Engineering and MS in Computer Science from Zhejiang University, China in 2002 and 2005 respectively. Current he is a PhD student in Arizona State University. His research interests are computer graphics and image processing.

DR. WONKA received his doctorate from the Technical University of Vienna in computer science. Additionally he received a Masters of Science in Urban Planning from the same institution. Prior to coming to ASU, he was a post-doctorate researcher at the Georgia Institute of Technology for two years. His research interests include various topics in computer graphics, especially real-time rendering and procedural modeling.

DR. ANSHUMAN Razdan is Associate Professor in the Division of Computing Studies and

the Director of Advanced Technology Innovation Collaboratory (ATIC) and the I³DEA Lab (i3deas.asu.edu) at Arizona State University at Polytechnic campus. He has been a pioneer in computing based interdisciplinary collaboration and research at ASU. His research interests include Geometric Design, Computer Graphics, Document Exploitation and Geospatial visualization and analysis. He is the Principal Investigator and a collaborator on several federal grants from agencies including NSF, NGA and NIH. He has a BS and MS in Mechanical Engineering and PhD in Computer Science. ar@asu.edu

JIUXIANG HU received the BS, MS and PhD degree in Mathematics from Huazhong Normal University in 1988, Huazhong University of Science and Technology, Wuhan, China, in 1991 and Lanzhou University, Lanzhou, China, in 1994, respectively. He is a research scientist in

Imaging and 3D Data Exploitation and Analysis (I3DEA) lab in the Division of Computing Studies at ASU Polytech campus and Partnership for Research in Spatial Modeling (PRISM) Lab at Arizona State University from 2000. His research interests include computer graphics, visualization, image processing and numerical computation. He has developed and implemented methods to segment biomedical volumedata sets, including image statistical and geometric modeling and segmentation techniques with application to structural and quantitative analysis of 2D/3D images.